DOI: 10.4408/IJEGE.2018-01.S-13

HIGH RESOLUTION 2D MODELLING OF RAPIDLY VARYING FLOWS: SOME CASE STUDIES

Paolo MIGNOSA, Renato VACONDIO, Francesca AURELI, Susanna DAZZI, Alessia FERRARI & Federico PROST

University of Parma - Dept. of Engineering and Architecture - Parco Area delle Scienze 181/a, 43124 Parma, Italy
Corresponding author: francesca.aureli@unipr.it

EXTENDED ABSTRACT

In natura si verificano molto spesso fenomeni alluvionali nei quali le grandezze caratteristiche del moto variano rapidamente nel tempo e/o nello spazio. Esempi tipici sono le alluvioni provocate da cedimenti strutturali di opere di ritenuta, i fenomeni propagatori generati da manovre brusche di organi mobili, i lahars a seguito di eruzioni vulcaniche, i tidal bores, onde a fronte ripido che si possono formare negli estuari soggetti a forti escursione di marea. Ai precedenti possono aggiungersi le esondazioni fluviali in zone caratterizzate dalla presenza di infrastrutture territoriali in rilevato o in zone urbanizzate, dove la dinamica dell'allagamento può essere influenzata in maniera assai sensibile dalla topografia. In tutti questi casi le simulazioni effettuate con modelli semplificati, il cui utilizzo è lecito per riprodurre fenomeni in cui il moto varia gradualmente, possono dar luogo ad approssimazioni generalmente non accettabili. A seconda dei fenomeni che si vogliono studiare, è quindi necessario disporre di un modello adeguato, in grado di rappresentare con accuratezza i fenomeni di interesse. Recentemente, l'utilizzo di modelli bidimensionali alle acque basse (2D-SWE), è diventato abbastanza comune per simulare i fenomeni di allagamento dovuti a esondazioni e/o crolli arginali, quando la modellazione monodimensionale non è in genere applicabile. I modelli espliciti ai volumi finiti, basati sui risolutori di Riemann, sono in grado di riprodurre adeguatamente l'evoluzione di un allagamento anche su una topografia accidentata, ma comportano ancora elevati tempi di calcolo laddove siano applicati su vasti territori e/o sia richiesta una elevata risoluzione spaziale. Tuttavia, le recenti tecniche di parallelizzazione MPI e GPU possono consentire di superare le limitazioni legate ai lunghi tempi computazionali, accelerando i calcoli anche di due ordini di grandezza e quindi permettendo di effettuare simulazioni di casi un tempo considerati proibitivi. Inoltre, l'uso di griglie non uniformi in codici GPU, oggetto di notevole attenzione nella recente letteratura scientifica, consente la modellazione di scenari di allagamento in aree vaste in cui sia richiesta una risoluzione spaziale molto elevata solo in porzioni limitate del dominio di calcolo.

Da lungo tempo ormai gli scriventi hanno elaborato uno schema numerico, accurato al secondo ordine nello spazio e nel tempo, implementato in ambiente CUDA e basato su una nuova tipologia di griglia, denominata BUQ (Block-Uniform-Quadtree), che consente di allocare in memoria solamente l'effettivo dominio di calcolo e di discretizzare il medesimo con risoluzione non uniforme. Nel presente lavoro, le potenzialità di tale modello vengono presentate attraverso i risultati della simulazione di due recenti fenomeni alluvionali verificatisi in Emilia. Il primo, verificatosi il 13 ottobre 2014 sui bacini dei torrenti Parma e Baganza, che vanno a confluire proprio nel centro della città di Parma, ha comportato l'allagamento di vasti quartieri della città stessa, in cui erano tra l'altro presenti un ospedale ed una centrale telefonica strategica per le comunicazioni in Emilia Romagna, con danni stimati in diverse decine di milioni di Euro. Viene anche descritto e messo in luce il ruolo benefico che ha avuto la cassa di espansione sul torrente Parma in occasione dell'evento e la potenziale dinamica dell'alluvione in caso la stessa non fosse stata realizzata ed in esercizio. Il secondo evento, verificatosi il 13 settembre 2015 sul torrente Nure, in provincia di Piacenza, ha provocato gravissimi danni all'abitato di Farini ed alle infrastrutture viarie della valle. È assai importante sottolineare che la ricostruzione di scenari di allagamento storici, conseguenti a piene a rapida evoluzione, può oggigiorno essere effettuata con confidenza cercando di sfruttare efficacemente i sempre più diffusi ed economici rilievi LiDAR ad elevata risoluzione spaziale. Come mostrato per questo tipo di simulazioni, la forte limitazione in termini di tempo di calcolo può essere almeno in parte superata. I nuovi codici paralleli e multirisoluzione, come quello qui impiegato, consentono infatti di simulare, con rapporti tra tempo fisico e tempo di calcolo assai elevati, allagamenti su territori di grande estensione, mantenendo nel contempo un'elevata risoluzione spaziale nelle zone di maggior interesse. Tali caratteristiche prospettano quindi la possibilità di applicazione a scala addirittura regionale. Si pensi ad esempio alla simulazione di scenari ipotetici di allagamento conseguente al cedimento di rilevati arginali, a scopo di Protezione Civile, oppure alle analisi volte alla conferma dell'adeguato comportamento di opere idrauliche di controllo delle piene già realizzate o alle necessarie analisi propedeutiche per valutare l'utilità e la tipologia di nuove opere idrauliche di difesa.

ABSTRACT

After a brief characterization of rapidly varying flows, a multi-resolution GPU-parallel numerical model implemented in CUDA/C++ for the solution of the 2D Shallow Water Equations is illustrated. Then, the activities developed with the aim of simulating two flooding events occurred in Emilia-Romagna (northern Italy) are detailed. The first event, happened on October 13th 2014 on the basin of the rivers Parma and Baganza, caused the flooding of wide districts of the town of Parma, with damages of several tens of millions of euros. The positive role of the river Parma flood detention reservoir during the event is also highlighted, as well as the possible consequences of the same event in the absence of the reservoir. The second event, occurred on September 13th 2015 on the river Nure (Piacenza), caused huge damages to the Farini village and to the Nure valley road infrastructure. The numerical simulations performed adopting the 2D high resolution numerical model allowed the correct reproduction of the real flooding events, with low computational time despite the high spatial resolution.

***Keywords**: 2D shallow water equations, rapidly varying flows, GPU-parallel numerical model, CUDA implementation, flooding scenario, flood detention reservoir*

INTRODUCTION

Fast flood events, in which the main flow variables (such as discharge, mean velocity, water depth, etc.) change rapidly in space and/or time, often occur in nature. Typical examples are the inundations due to dam or levee breaking or breaching, the rapidly varying flows induced by the operation at dam outlet facilities, the sudden mudflows or debris flows consequent to volcanic eruptions (*lahars*), the surges and bores that can travel up a river mouth due to high tides (Chanson, 2012). Flood inundations in areas characterized by the presence of roads, railways or channel embankments, or in urban environments, where the flooding dynamics can be strongly influenced by the streets and the buildings, can also be ascribed to this category. In all these cases, the simulations performed with simplified models, neglecting some of the terms of the momentum equations, can give rise to unacceptable approximations.

In order to quickly evaluate the consequences of neglecting some of the terms of the momentum equation, let us consider the simple 1D Shallow Water Equations (SWE) written for a rectangular channel in a conservative form:

$$\frac{1}{g}\frac{\partial u}{\partial t}+\frac{u}{g}\frac{\partial u}{\partial x}+\frac{\partial \eta}{\partial x}+S_f=0 \qquad (1)$$

in which u is the water velocity, $\eta=h+z$ is the free surface elevation above a datum, (h being the water depth and z the bed elevation), S_f is the friction slope, g is the gravitational acceleration, x is the distance along the channel and t is the time. In the non-dimensional form of eq. 1 each term represents a slope (Cunge *et alii*, 1980). The first two terms (*inertial terms* or *acceleration slopes*) represent the slope due to the variation of velocity in time and the slope corresponding to the variation of the velocity head in space, respectively. The third term is the slope of the water surface itself, while the fourth represents the friction slope. For gradually varying flows, characterized by mild variations in space and time, the first two terms in eq.1 can be one or two orders of magnitude smaller than the slopes of the water surface and friction, and can be neglected.

For example, let us consider the rising limb of a flood in a wide alluvial river, such as the Po river in its middle reach. In this case, the mean velocity can vary up to 0.1 m/s in 1 hour in the same cross section and from 1.8 to 1.3 m/s between two cross sections 32 km far apart (maximum values observed in the rising hydrographs of the May 2002 flood event between Boretto and Borgoforte).The first two terms of eq. 1 then become:

$$\frac{1}{g}\frac{\partial u}{\partial t}\approx\frac{1}{9.81}\frac{0.1}{3600}\approx 2.8\cdot10^{-6}\quad \frac{u}{g}\frac{\partial u}{\partial x}=\frac{\partial\left(\frac{u^2}{2g}\right)}{\partial x}\approx\frac{\left(\frac{1.69-3.24}{2\cdot9.81}\right)}{32000}\approx-2.5\cdot10^{-6}$$

while the water surface slope is about 2×10^{-4}, that is two orders of magnitude greater. In this case, neglecting the first two terms of eq. 1 (*parabolic scheme*) can lead to acceptable approximations.

Let us now consider the case of a sudden release of the water stored in a reservoir due to an instantaneous dam collapse in a frictionless horizontal channel of rectangular cross section. The analytical solution of the 1D Saint Venant equations for the dry-bed case in the presence of an initial depth h_0 in the reservoir was provided by Ritter (1892) and has the form:

$$\begin{cases} u=\dfrac{2}{3}\left(\sqrt{g\cdot h_0}+\dfrac{x}{t}\right) \\ h=\dfrac{1}{9\cdot g}\left(2\cdot\sqrt{g\cdot h_0}-\dfrac{x}{t}\right)^2 \end{cases} \qquad (2)$$

where x is a positive abscissa with origin at the dam section. The terms of eq. 1 then become:

$$\begin{cases} \dfrac{1}{g}\dfrac{\partial u}{\partial t}=\dfrac{1}{g}\left[\dfrac{2}{3}\left(-\dfrac{x}{t^2}\right)\right] \\ \dfrac{u}{g}\dfrac{\partial u}{\partial x}=\dfrac{\dfrac{2}{3}\left(\sqrt{g\cdot h_0}+\dfrac{x}{t}\right)}{g}\left[\dfrac{2}{3}\left(\dfrac{1}{t}\right)\right] \\ \dfrac{\partial \eta}{\partial x}=\dfrac{\partial h}{\partial x}=\dfrac{2}{9\cdot g}\left(2\cdot\sqrt{g\cdot h_0}-\dfrac{x}{t}\right)\left(-\dfrac{1}{t}\right) \end{cases} \qquad (3)$$

Setting g to 10 m/s^2 and h_0 to 10 m (so that $(gh_0)^{0.5}$ gives 10 m/s) and considering a cross section 50 m downstream of the dam (five times the initial water depth h_0) 5 seconds after the collapse, the terms in eq. 3 become:

$$\frac{1}{g}\frac{\partial u}{\partial t}=-0.1\overline{3};\quad \frac{u}{g}\frac{\partial u}{\partial x}=0.1\overline{7};\quad \frac{\partial \eta}{\partial x}=\frac{\partial h}{\partial x}=-0.0\overline{4}$$

In this case, the first two terms of eq.1 are greater than the third one (and obviously than the fourth, the friction slope *Sf,* that in this ideal case is equal to zero) and cannot be neglected to achieve a correct numerical solution.

All these considerations lead to the obvious conclusion that the model adopted for a numerical simulation has to be suitable for solving the particular phenomenon of interest. Of course, a complete model can be adopted in any situation, provided that the river geometry is sufficiently well known. Nowadays, due to the efficiency of modern computers, the computational burden is no more a problem, at least for 1D simulations, and simplified approaches, very popular until a few years ago, tend to be restricted inside rainfall-runoff hydrological models, or in case the river geometry is only approximately known.

Different is the case of 2D Shallow Water Models, that are now fairly common for the simulation of dam or levee break inundations if the 1D schematization is not acceptable (Valiani *et alii*, 2002; Aureli & Mignosa, 2004; Costabile & Macchione, 2015; Vacondio *et alii*, 2016). Explicit Finite Volume (FV) models, based on Riemann solvers, are suitable for solving most of the phenomena that can occur during this kind of flood events, but, unfortunately, they are still computationally expensive if applied to wide regions and if a high spatial resolution is required. To overcome this issue, parallel numerical schemes based on MPI or GPU techniques have been recently developed, allowing to perform otherwise prohibitive simulations thanks to the high ratios between physical and computational times (Vacondio *et alii*, 2014). However, most of the GPU-accelerated models are based on uniform Cartesian grids, which have two major limitations: (i) the same resolution has to be adopted in the whole domain, and (ii) the shape of the domain has to be rectangular. The adoption of non-uniform grids has recently gained attention in literature (Lacasta *et alii*, 2014; Lacasta *et alii*, 2015a, b; Juez *et alii*, 2016; Vacondio *et alii*, 2017). The possibility of adopting high-resolution and multiresolution grids allows an accurate description of the topography even in those areas where the presence of embankments can strongly influence the flooding dynamics. Sometimes these linear or sub-linear elements are treated as 1D through internal boundary conditions, assuming a perpendicular flow in case of their overtopping (Altinakar *et alii*, 2009, Miglio *et alii,* 2008). However, this kind of schematization leads to a very complex model setting, and prevents from the correct modelling of local phenomena that can occur at the propagation of flooding fronts. As an example, in Fig. 1 the flow field (water depths and velocities) near a cloverleaf road interchange is shown: all the ramps were represented and modelled at a high spatial resolution, in a pure 2D model.

After a brief description of the PARFLOOD 2D numerical model developed by the University of Parma, the results of the simulation of two different flooding events recently occurred in Emilia-Romagna are presented.

NUMERICAL MODEL

The PARFLOOD numerical model solves, through a Finite Volume scheme, the 2D-SWE written in the integral form (Toro, 1999a):

$$\frac{\partial}{\partial t}\int_A \mathbf{U}\,dA + \int_C \mathbf{H}\cdot\mathbf{n}\,dC = \int_A \left(\mathbf{S}_0 - \mathbf{S}_f\right)dA \tag{4}$$

where A is the area of the integration element, C is the element boundary, n is the outward unit vector normal to C, U is the vector of the conserved variables, $H = (F, G)$ is the tensor of fluxes in the x and y directions, S_0 and S_f are the bed and friction slope source terms, respectively. In the model, the modified form of SWEs proposed by Liang & Borthwick (2009) is adopted:

$$\mathbf{U} = \begin{bmatrix} \eta \\ uh \\ vh \end{bmatrix},\ \mathbf{F} = \begin{bmatrix} uh \\ u^2h + \frac{1}{2}g\left(\eta^2 - 2\eta z\right) \\ uvh \end{bmatrix},$$
$$\mathbf{G} = \begin{bmatrix} vh \\ uvh \\ v^2h + \frac{1}{2}g\left(\eta^2 - 2\eta z\right) \end{bmatrix},\ \mathbf{S}_0 = \begin{bmatrix} 0 \\ -g\eta\frac{\partial z}{\partial x} \\ -g\eta\frac{\partial z}{\partial y} \end{bmatrix} \tag{5}$$

in which h is the flow depth, u and v are the velocity components in the x and y directions, g is the gravitational acceleration, z is the bed elevation, and $\eta = h + z$ is the free surface elevation above datum. The slope source term is discretized using a centered approximation (Vacondio *et alii*, 2014), but the main advantage of the modified version of the SWEs reported in eq.

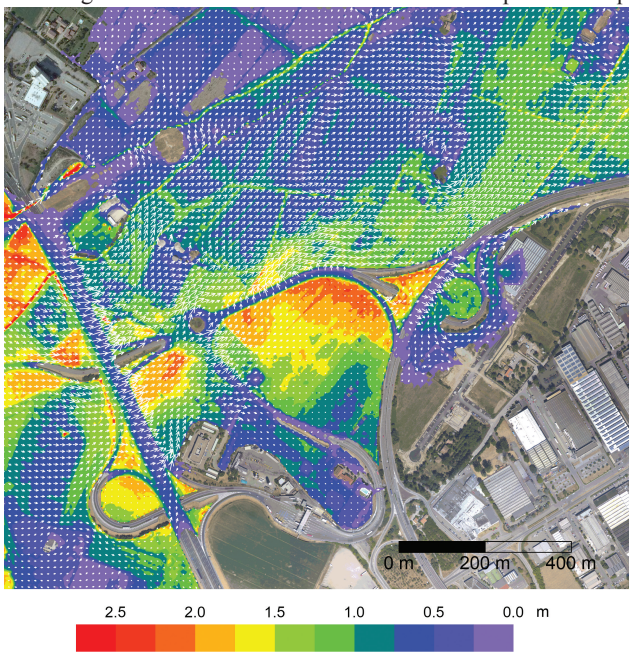

Fig. 1 - Flow field due to levee breaking near a cloverleaf road interchange

5 is that it guarantees the C-property, defined as the capability of preserving still water at rest (Vázquez-Cendón, 1999), regardless of the adopted discretization form of the slope source term. The procedure proposed by Liang & Marche (2009) for 1D uniform grids has been extended in the present work to guarantee the C-property also in presence of 2D non-uniform grids. The friction source term is based on the Chezy-Manning equation, and it is discretized using the implicit formulation proposed by Caleffi *et alii* (2003) to avoid instabilities at small water depths. Fluxes are calculated using a HLLC approximate Riemann solver, and second order accuracy in space is ensured by adopting a Monotone Upwind Schemes for Scalar Conservation Laws (MUSCL) interpolation with minmod limiter (Toro, 1999b). The model is implemented in a CUDA/C++ code that exploits parallel computation offered by modern GPU video cards. In CUDA, the basic work unit is represented by a thread and many threads are grouped into blocks (NVIDIA, 2007). In the present model each thread corresponds to a computational cell used to discretize the physical domain, and M×M cells form a regular block. Each block of data can be processed in parallel by a multicore of the GPU taking advantage of fast memory communication, which is fundamental for cell neighborhood information exchange.

In order to achieve high computational efficiency, many optimization procedures were adopted as to minimize the information exchange between CPU and GPU: as an example, all the computations are performed on the GPU, and the conserved variables arrays are transferred to the CPU only at the required output time. Another reduction of computational times was achieved focusing on the adopted computational grid type. Most of the GPU codes make use of Cartesian grids (Vacondio *et alii*, 2014), in which data are stored as a simple two-dimensional array, and therefore cell neighbors localization in memory is straightforward. To preserve the computational organization of the grid in blocks in case different resolution levels need to be used, a new type of grid named Block-Uniform Quadtree (BUQ) was introduced. The domain is still partitioned into blocks, each containing M×M cells with uniform spatial resolution within the block, but cells belonging to different blocks can be characterized by a different spatial resolution level: level 1 with cell size Δ_1, level 2 with cell size $\Delta_2=2\times\Delta_1$, up to level n with cell size $\Delta_n=2^{n-1}\times\Delta_1$. M is assumed equal to 8 or 16, but it can be assumed equal to any power of two. This organization requires a different type of memory storage of the multiresolution grid: blocks with various resolutions are tiled according to their code index, and therefore the original block proximity is not maintained in the final tiling. Additional information allows to retrieve the original position in the grid, its resolution and the index of neighboring blocks during the computations. For more information about the code, see Vacondio *et alii* (2014, 2016, 2017).

MODELLING OF THE FLOODING OF PARMA AND EVALUATION OF THE EFFECT OF THE RIVER PARMA FLOOD DETENTION RESERVOIR

Event description

During October 13th 2014, a wide convective front coming from south-west brought heavy rainfall across the Parma and Baganza watersheds (Fig. 2) with maximum amounts up to 200-250 mm in the gauging stations of the Apennine ridge and durations between 3 and 9 hours, quite critical because close to the concentration times of the basins.

Table 1 contains the top values, ranked in decreasing order, of maximum historical rainfall events in 1-24 hours at Marra gauging station (upper Parma valley). It can be easily noticed that the rainfall event of October 13th 2014 was by far the maximum in the historical data record (57 years) for all the considered durations, reaching almost twice the values of the second maximum for 3 and 6 hours.

As a further proof of the exceptionality of the rainfall event, Fig. 3 shows the Depth-Duration-Frequency (DDF) relationships for two different gauging stations belonging to the Parma and Baganza river watersheds (Marra and Calestano, respectively), together with the maximum rainfall amounts observed during the

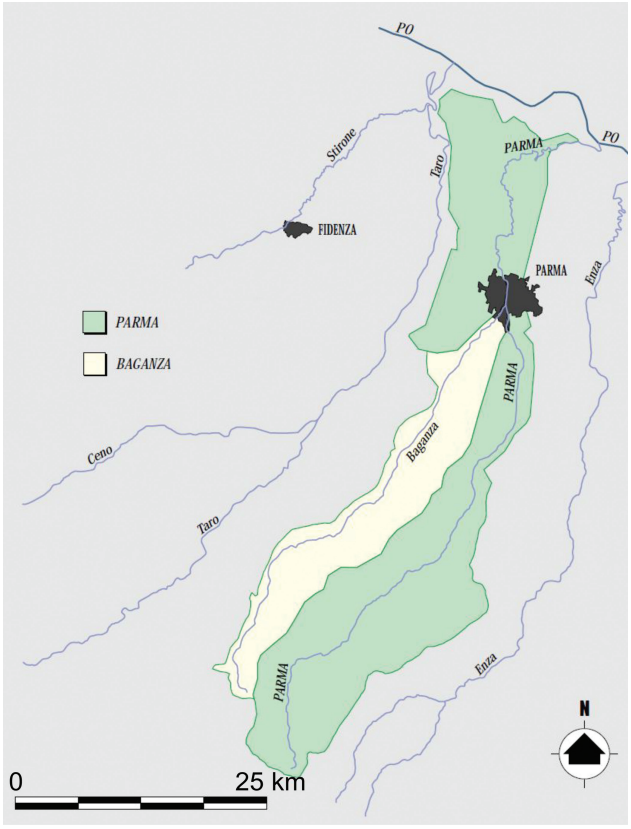

Fig. 2 - Parma and Baganza watersheds (from PAI)

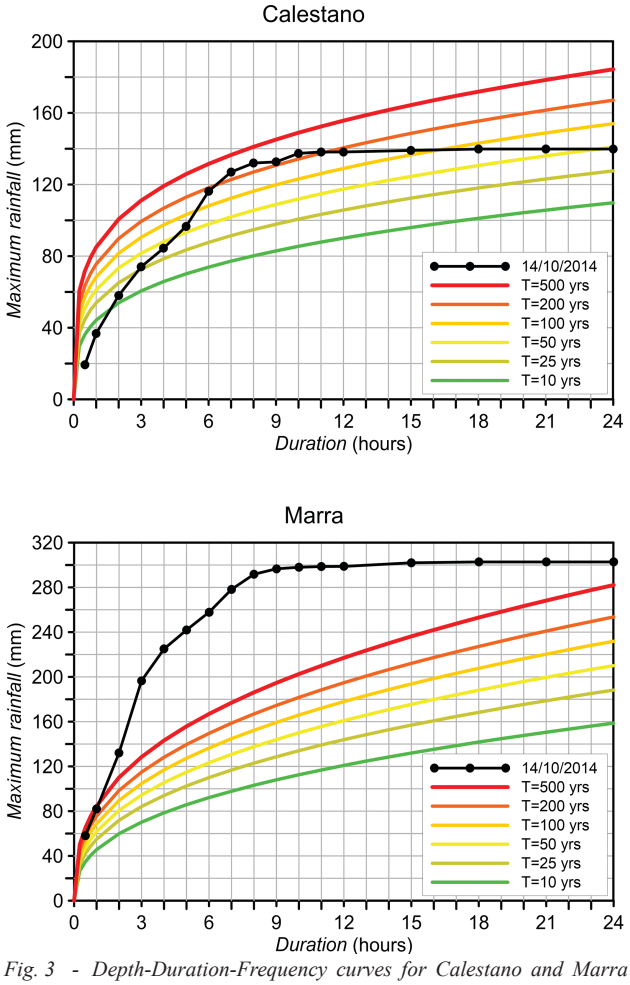

Fig. 3 - Depth-Duration-Frequency curves for Calestano and Marra gauging stations and maximum rainfall observed for the October 13th 2014 event

October 13th 2014 event.

For Marra gauging station, all the recorded values are far above the 500 years DDF curve, such that a reasonable statistical characterization of the considered rainfall event is quite difficult. Also for Calestano gauging station, the maximum observed rainfall amounts, for durations between 6 and 10 hours, are slightly above the 200 years DDF. Despite the high infiltration capacity of the soils due to a long antecedent dry period, these heavy rains explain the consequent catastrophic flood occurred on the Baganza river.

During the flood event, water levels were recorded at three gauging stations along the Baganza and Parma rivers. In Table 2, the distance between two consecutive gauging stations and the measured peak travel time, together with the calculated peak celerity, are shown. Upstream of the city of Parma, between Marzolara and Ponte Nuovo gauging stations, the flood peak propagated with a celerity of 5.2 ms^{-1}, taking only 1 hour and 10 minutes to travel a distance of about 22 km.

This event caused the partial inundation of the Parma city, due to the insufficient conveying capacity of the urban reach of the Baganza river. A historical pedestrian bridge (Fig. 4a) was destroyed and huge damages occurred to very important settlements (one hospital, the main regional telephone exchange) and residential neighborhoods (Fig. 4b), estimated at several tens of millions of euros. Actually, it was well known that the urban reach of the Baganza river was not capable to deliver high return period flows; in fact, a flood control reservoir has been in study for many years. Also the urban reach of the Parma river, downstream of the confluence with Baganza river, was put to the test by the flood wave with minimization of the freeboard (Fig. 4c and 4d), and gave origin to a local, and fortunately small, flow overtopping of the river levee, with an incipient breaching quickly fixed by the local hydraulic authority (Fig. 5).

The flood detention reservoir on the Parma River

The flood detention reservoir on the Parma river (Fig. 6) is located a few kilometers upstream of the homonymous town. The reservoir is in line with the river course, and the dam is composed of a central straight body with two lateral duckbill spillways (Fig. 7a), which aim at significantly increasing the length of the spillway, while limiting the overall width of the dam. The central portion of the dam is equipped with three movable plain gates at the bottom outlets.

During the event under consideration, the reservoir played a key role in the mitigation of the flood wave travelling downstream towards the city of Parma. Thanks to the real-time regulation of the gates at the bottom outlets, the reservoir was capable

Ranked position	*year*	*1 hour*	*year*	*3 hours*	*year*	*6 hours*	*year*	*12 hours*	*year*	*24 hours*
1	***2014***	**81.8**	***2014***	**196.6**	***2014***	**257.0**	***2014***	**298.6**	***2014***	**302.8**
2	*1980*	61.4	*1973*	102.6	*1980*	129.0	*1980*	166.0	*1980*	207.8
3	*1973*	59.4	*1997*	93.6	*1997*	123.6	*1948*	162.0	*2012*	199.6
4	*1948*	54.0	*1994*	78.4	*2012*	105.4	*2012*	160.6	*1948*	182.0
5	*1945*	45.0	*1980*	77.2	*1973*	104.6	*1994*	160.0	*1997*	175.0
6	*1994*	44.4	*2004*	71.6	*1986*	104.2	*1997*	143.8	*2011*	174.4
7	*1997*	44.2	*2011*	68.4	*1965*	101.8	*2011*	140.4	*1945*	170.0
8	*1965*	39.6	*1986*	68.0	*1948*	100.0	*1973*	121.2	*1994*	160.2

Tab. 1 - Maximum historical rainfall depths (mm) for 1-24 hours recorded at Marra gauging station (57 years)

Reach		***Length (km)***	***Travel time (hours:min)***	***Wave celerity (m/s)***
Baganza at *Marzolara g. s.*	Baganza at *Ponte Nuovo g. s.* (city)	22.0	1:10	5.2
Baganza at *Ponte Nuovo g. s.* (city)	Parma at *Ponte Verdi g. s.* (city)	1.85	0:20	≅1.5
Parma at *Ponte Verdi g. s.* (city)	Parma at *Colorno g. s.*	33.2	10:00	0.92

Tab. 2 - Parma and Baganza river reaches between two subsequent water level gauging stations: length of the reach, travel time and wave celerity for the peak of the October 13th 2014 event

Fig. 4 - October 13th 2014 flood event: a) initial phases of the historical pedestrian bridge collapse; b) residential neighborhoods flooded by the Baganza river; c) urban reach of the river Parma downstream of the confluence with the Baganza river; d) bridge piers with wood debris

Fig. 5 - Incipient breaching in the river Parma levee

of storing about $8.3 \cdot 10^6$ m^3 of water (the maximum retainable volume at the dam crest is $10 \cdot 10^6$ m^3). The huge amount of driftwood coming from upstream was almost completely kept by the dam (Fig. 7b). Fig. 8 shows the total outflow discharge at the bottom gates, the water level in the reservoir, and the inflow into the reservoir as a function of time. On the top, the time history of the gate openings is also shown.

The outflow discharge time series was computed from the stage-discharge-gate opening relationships obtained by the Authors through a laboratory investigation on a scale physical model of the dam in 2008 (Dicatea, 2008). The total inflow discharge into the reservoir was estimated on the basis of the water levels in the reservoir and of the outflow at the bottom gates through a Bayesian inverse procedure developed by D'Oria *et alii* (2012). This technique has the advantage of minimizing the spurious oscillations that could affect the hydrograph due to the sudden changes in the outflow, caused by the controlling of the gates, and to the irregularities in the water level records due to unavoidable uncertainties at the water level gauge site on the dam. The peak of the inflow hydrograph was estimated to be about 950 m^{3}s^{-1}, while the outflow hydrograph shows a peak of about 300 m^{3}s^{-1}.

Based on the above considerations, it is already manifest that the Parma river flood detention reservoir played a key positive role in protecting the city of Parma and the whole river system from further flooding that could have been devastating in its absence. This will be further discussed in the following sections.

Fig. 6 - Aerial view of the flood detention reservoir on the Parma river during the filling tests in 2008

Fig. 7 - Aerial view of the dam (top), accumulation of the driftwood at the right duckbill spillway and condition of the reservoir at 18:13 of October 13th 2014 (bottom)

Numerical modelling

Figure 9 shows the Parma and Baganza confluence along with the urban area prone to flooding. The numerical simulations were performed adopting the PARFLOOD model previously described. The domain was discretized adopting 1 m × 1 m square cells on the basis of a DTM produced by the local company CGR S.p.A after a LiDAR survey realized a few days after the event, and donated free of charge to the city of Parma for study purposes. The bathymetry was then integrated with data obtained from local surveys performed by the local agency "Servizio Tecnico dei Bacini degli affluenti del fiume Po" (STB) in order to achieve a better accuracy in those areas in which the digital removing of man-made and other features from the DSM can give origin to inaccuracies (say, as an example, the presence of high growing and dense vegetation that can cause the lack of ground data).

Among the different techniques that account for the influence of the buildings on the flooding dynamics (Schubert & Sanders, 2012), the building-resistance strategy was favored. This approach represents the footprint of buildings and other structures with a higher resistance (Manning) coefficient, and was preferred to the building-hole approach (i.e. the computational mesh is generated with holes inside the building footprints), since most building basements were actually flooded due to the presence of lowered surrounding yards. The mesh was composed of about $6.76 \cdot 10^6$ potentially floodable cells.

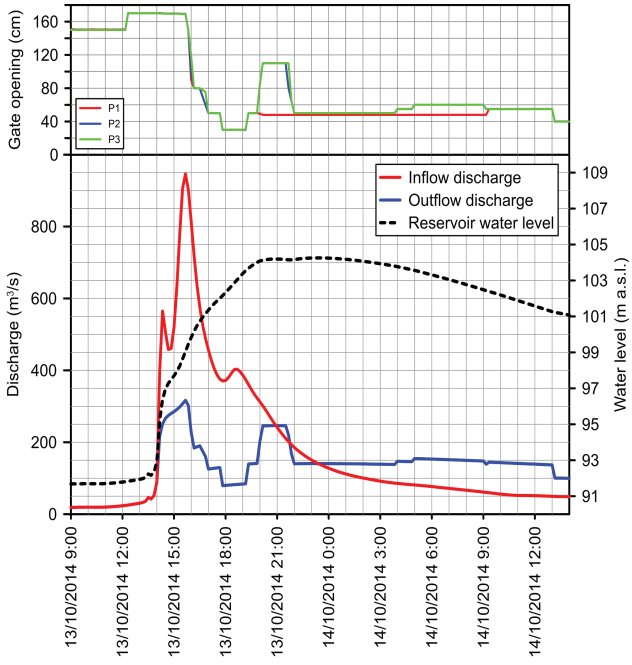

Fig. 8 - Water levels, inflow and outflow discharges at the Parma river flood detention reservoir during the October 13th 2014 flood event

Fig. 9 - Aerial view of the modelled area

Simulations and results

The following boundary conditions (b.c.) were assumed:

1. The upstream b.c. for the Baganza river was the discharge time series obtained by routing the recorded hydrograph at Marzolara gauging station (22 km upstream) through an 1D SWE model;
2. The upstream b.c. for the Parma river was the discharge time series obtained by routing the outflow from the Parma river dam, through an available 1D SWE model of the Parma river;
3. As downstream b.c. on the Parma reach, the water level time series recorded at Ponte Verdi gauging station (downstream of the confluence with the Baganza river) was imposed.

The flood event was modelled from 12:00 a.m. to 8:00 p.m. of October 13th 2014, and, thanks to the GPU implementation, the simulation runtime was approximately 4.5 hours adopting a NVIDIA Tesla® K40 device.

Figure 10 shows the map of the maximum (non-simultaneous) water depths and of the flooded area obtained from the numerical modelling (HYLAB-DICATEA, 2014), together with the boundary of the area that was actually flooded. The numerical simulation reproduced both the areas in which the levees were overtopped and the whole area subject to flooding quite well. However, differences can be observed in some areas (A, B and C in Fig. 10). Flooding is slightly overestimated in the areas identified with A and C, although water depths are lower than 0.1 m, while the numerical modelling underestimates the flooded area in B. A reason can be identified in the DTM possible inaccuracies in describing all the features of urban areas (SAMPSON *et alii*, 2012), such as curbs and low-height slurry walls. Also the presence of the vegetation canopy can often represent an important source of error due to the limits of the common LiDAR vegetation point

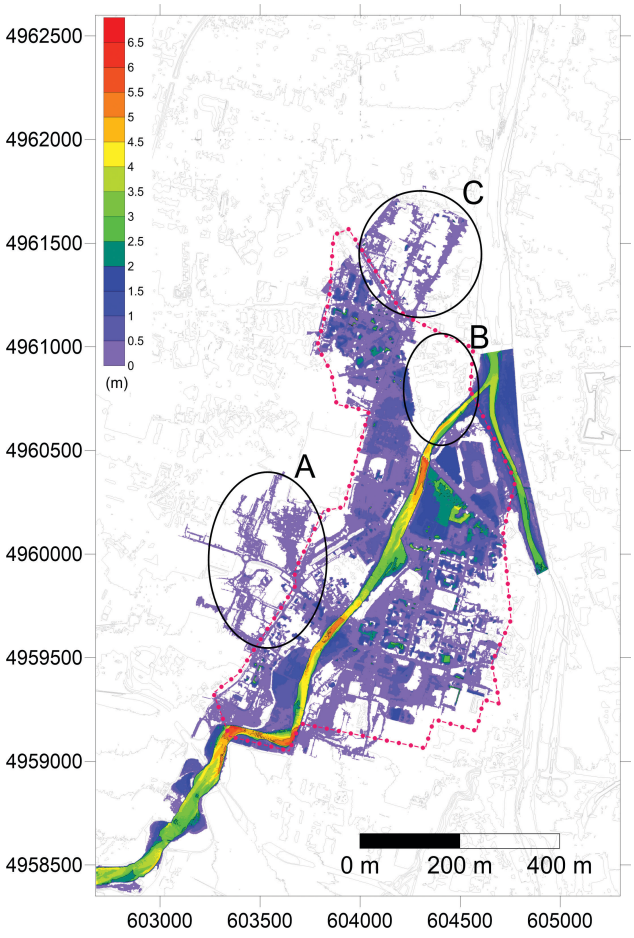

Fig. 10 - Maximum water depths obtained through the numerical modelling

removal algorithms (Raber *et alii*, 2002). Moreover, all these inaccuracies are usually scarcely controllable by the modeler. Despite the integration of the DTM with additional ground data, the accuracy in the elevation remains around 0.10-0.15 m: such values are comparable with the computed (or missing) water depths. Another reason can be found in the approach adopted for the description of buildings and of their water storage capability, not satisfactorily described through the *building-resistance* strategy. Finally, uncertainties are also present in the upstream boundary condition of the Baganza river reach, due to approximations in the stage-discharge relationship at Marzolara gauging station.

Figure 11 shows the computed flow field near the "*chicane*" of the Baganza river at the town entrance. On the outside of the two curves, where the flow coming from upstream is forced to change direction abruptly, water elevations calculated by the model are more than 1 m higher than on the inside. This behavior could not have been caught adopting 2D simplified numerical models in which the inertia terms are neglected, nor through the use of 1D models that assume a horizontal distribution of the profile in each cross section. At these locations the levees are partially overtopped, and gave origin to the inundation of the surrounding neighborhood, on both sides. Overtopping occurs also downstream, due to the narrowing of the river reach.

Simulations in the absence of the river Parma flood detention reservoir

Fig. 8 highlights the important effect of the Parma detention reservoir in dampening the outflow flood hydrograph during the October 13th 2014 flood event. It seemed therefore interesting to analyze the harmful consequences that the absence of the flood detention reservoir could have entailed during this event. For this reason, another flooding scenario was investigated, adopting as upstream boundary condition for the Parma river reach the flood wave entering the reservoir (Fig. 8), obtained through the Bayesian reverse approach. Due to the obvious lack of correspondent records at the Ponte Verdi gauging station, and also with the aim of moving the boundary condition far away from the confluence, the modeled river reach was prolonged about 1 km downstream and a stage-discharge relationship was imposed at the railway bridge. Figure 12 shows the maximum (non-simultaneous) water depths at the end of the simulation (from 12:00 a.m. to 10:00 p.m. of October 13th 2014) for this new flooding scenario. It can be quickly recognized that the computed flooded area now also includes the city center both to the left and to the right sides of the Parma river, as well as all the areas flooded in the previous scenario. These results underpin the positive role exerted by the Parma river flood detention reservoir, along with the importance of a correct real-time regulation of its gates.

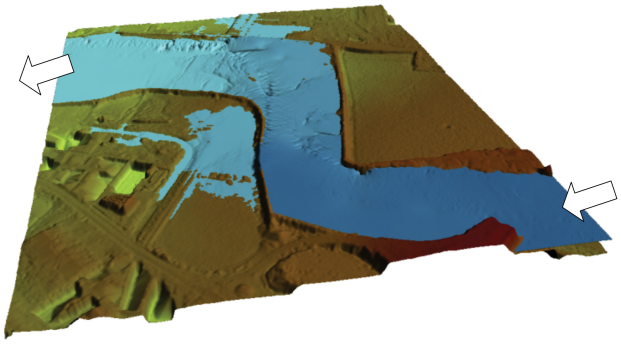

Fig. 11 - Modelling of the initial phase of the flooding near the chicane in which the Baganza river is forced at the entrance of the town of Parma

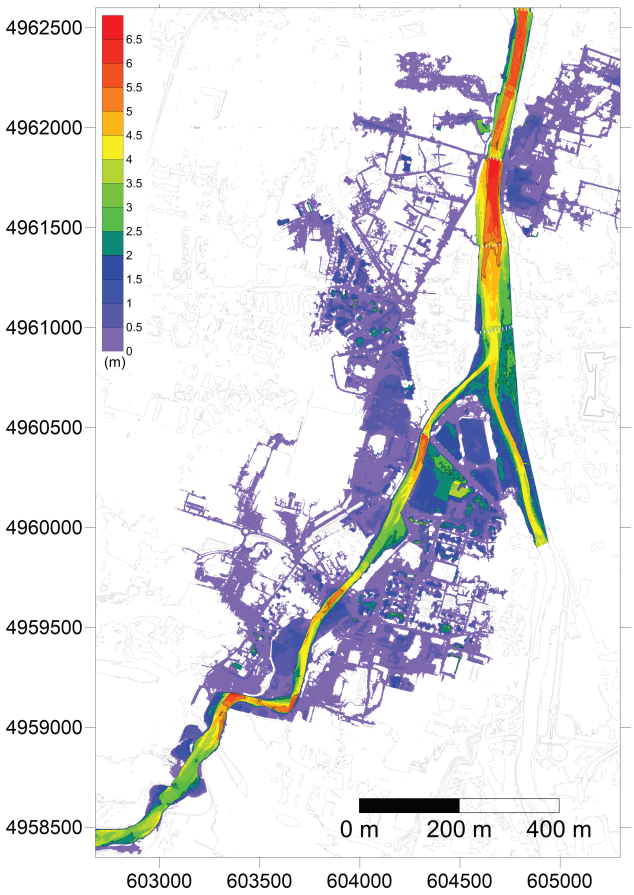

Fig. 12 - Maximum water depths for the second considered flooding scenario

MODELLING OF THE EVENT OF SEPTEMBER 13TH -14TH 2015 ON THE RIVER NURE

Event description

During the night between September 13th and 14th 2015, a wide convective front coming from south-west brought heavy and extensive rainfalls on the Western Emilia-Romagna

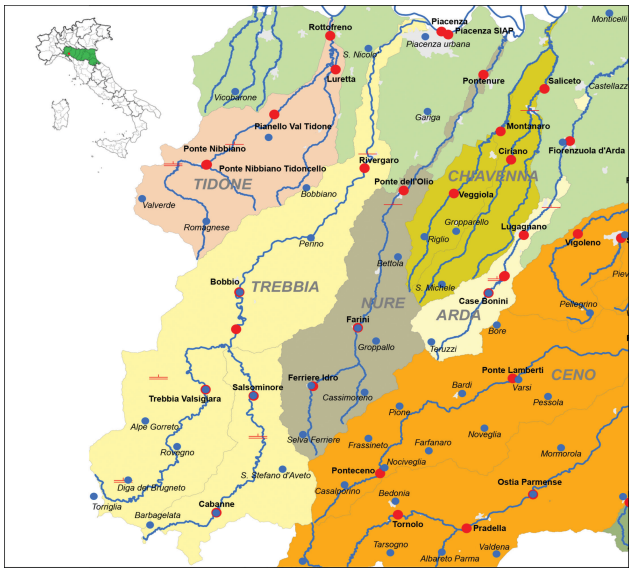

Fig. 13 - Watersheds of the rivers Trebbia and Nure with water depth (red) and rainfall (blue) remote control gauging stations (ARPAE, 2015)

Apennine region, striking especially the Trebbia and Nure river watersheds (Piacenza) (Fig. 13). The raingauges located in the two mentioned watersheds recorded very high hourly rainfall intensity (>100 mm·h^{-1} at 5 stations and >80 mm·h^{-1} at 10 stations) (ARPAE, 2015).

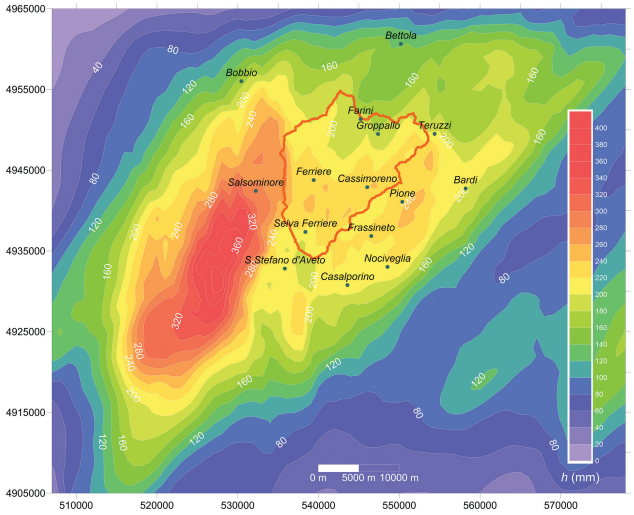

Fig. 14 - Isohyet map of total rainfall h for the event of interest obtained through the radar reflectivity, linked to rain gauges

The upper part of the Nure river basin (208 km^2 at the Farini outlet) was seriously hit. Figure 14 shows the Isohyet map of the total rainfall obtained by the reflectivity field acquired by the Gattatico (RE) meteorological radar, linked to rain gauges (Fornasiero *et alii*, 2008). Even if the eye of the rainfall event is located south-east, values above 250 mm were observed over the upper part of Nure river basin, with an estimated total rainfall volume of about 45·10^6 m^3. The rainfall event gave

Fig. 15 - Farini village before (top) and after (bottom) the flooding event of September 13th -14th 2015

origin to an exceptional flood that brought devastation to the whole Nure river valley, destroying many buildings located along the river, especially in the village of Farini (Fig. 15), the main valley road, and damaging the Sassi Neri check dam built to protect the river course from a landslide that tends to obstruct the valley (Fig. 16).

In the following days, several survey campaigns were carried out. An unmanned aerial vehicle captured ground images at the resolution of 10 cm/pixel, a LiDAR survey and a 1×1 m DTM of a significant portion of the river valley were produced by CGR S.p.A, and a traditional ground survey was conducted in order to identify the maximum levels reached by the water into the village and upstream.

Clear marks of the mud and debris, more than 11 meters above the valley floor, were observed upstream of the narrow section of the Sassi Neri check dam. These signs allowed to identify a posteriori the occurrence, just for few night hours, of an ephemeral lake.

Fig. 16 - The Sassi Neri check dam after the flood event (from downstream). The flow circumvented and damaged the structure on the left

Numerical modelling

A 2.6 km long reach of the river and valley, ranging from the upstream end of the ephemeral lake down to a check dam present in the river course immediately downstream the village of Farini (Fig. 17a), was modelled.

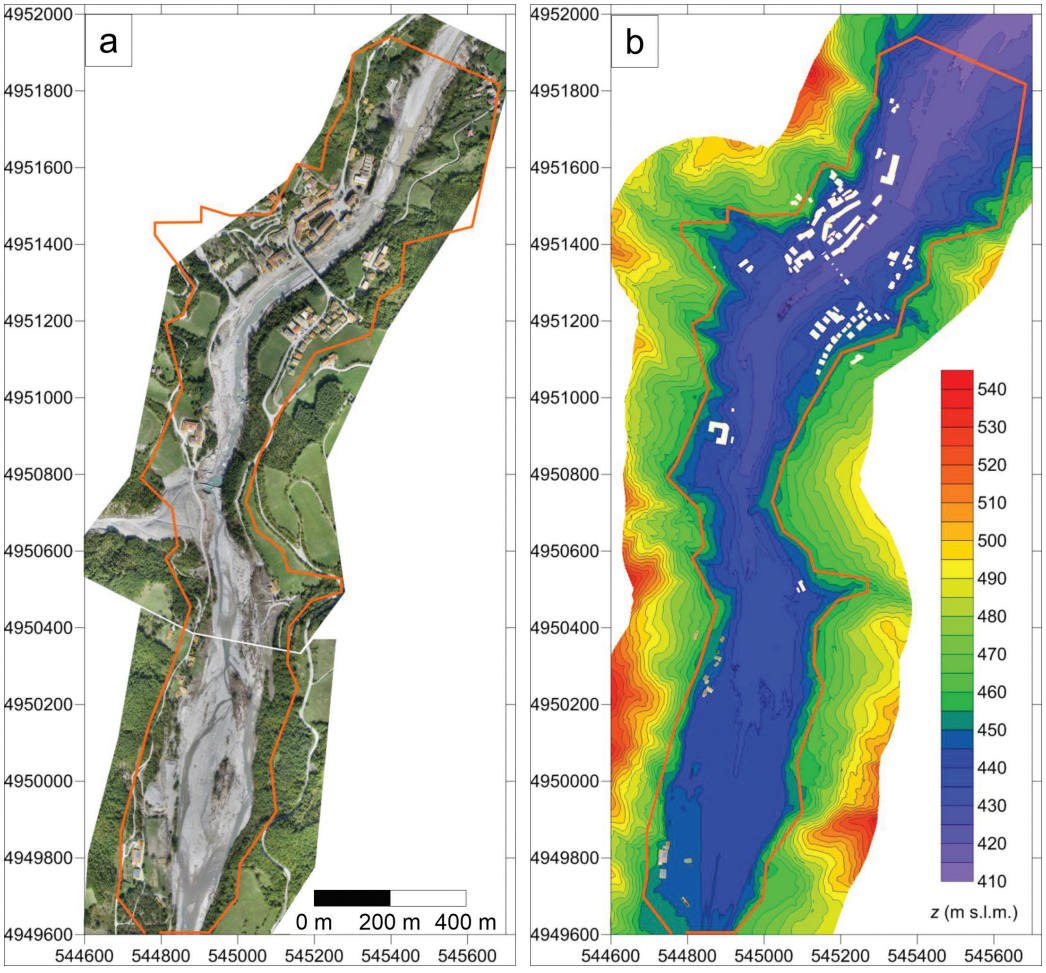

Fig. 17 - Modelled area (a) and bathymetry (b)

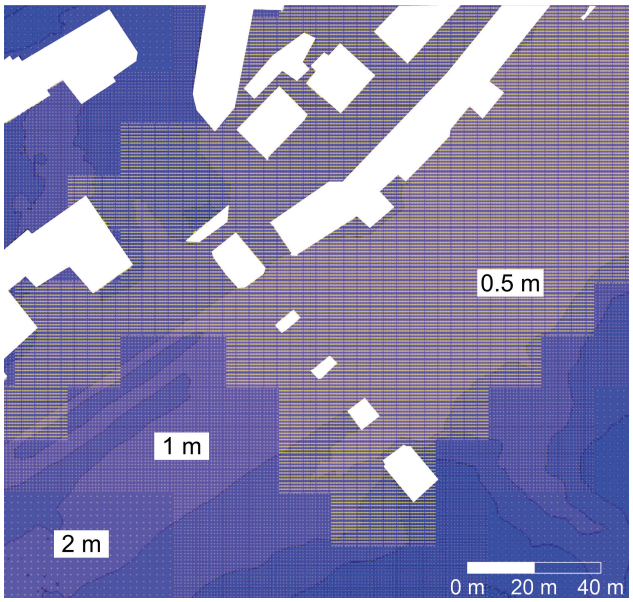

Fig. 18 - Detail of the BUQ multiresolution computational grid near the village of Farini

With the aim of accurately describing all the structures present in the built-up area, a 0.5×0.5 m square grid was firstly obtained from the bilinear interpolation of the available DTM of 1×1 m ($3.428 \cdot 10^6$ active cells) and then refined by means of the ground surveys as to retain some planimetric and altimetric features of the structures. Since the numerical simulation was performed adopting the PARFLOOD model and BUQ grids, in the computational domain, the highest resolution (0.5×0.5 m cells) was maintained only in the areas of interest (village of Farini, zone of the bridge, confluences, etc.), whereas it was decreased up to 2 m where a lower accuracy was considered adequate. As a result, the multiresolution computational grid was composed of $0.974 \cdot 10^6$ active cells, with a variable resolution of 0.5, 1 and 2 m (Fig. 18).

In order to obtain a detailed description of the flow field in the urban area, the building-hole methodology (Schubert & Sanders, 2012) was adopted to model the buildings; in this approach the grid cells that fall inside the footprint of buildings are considered inactive (Fig. 17b) and excluded from the calculation.

Simulations and results

Due to the lack of water level rain gauges, the discharges coming from the Nure river and from the main three lateral tributaries were reconstructed by means of a distributed hydrological model. Spatial and time distribution of the rainfall was derived from the 15 minutes reflectivity fields acquired by the meteorological radar, linked to the rain gauges (Mignosa *et alii*, 2015). The resulting flood hydrographs were imposed as upstream boundary conditions for the Nure river and the

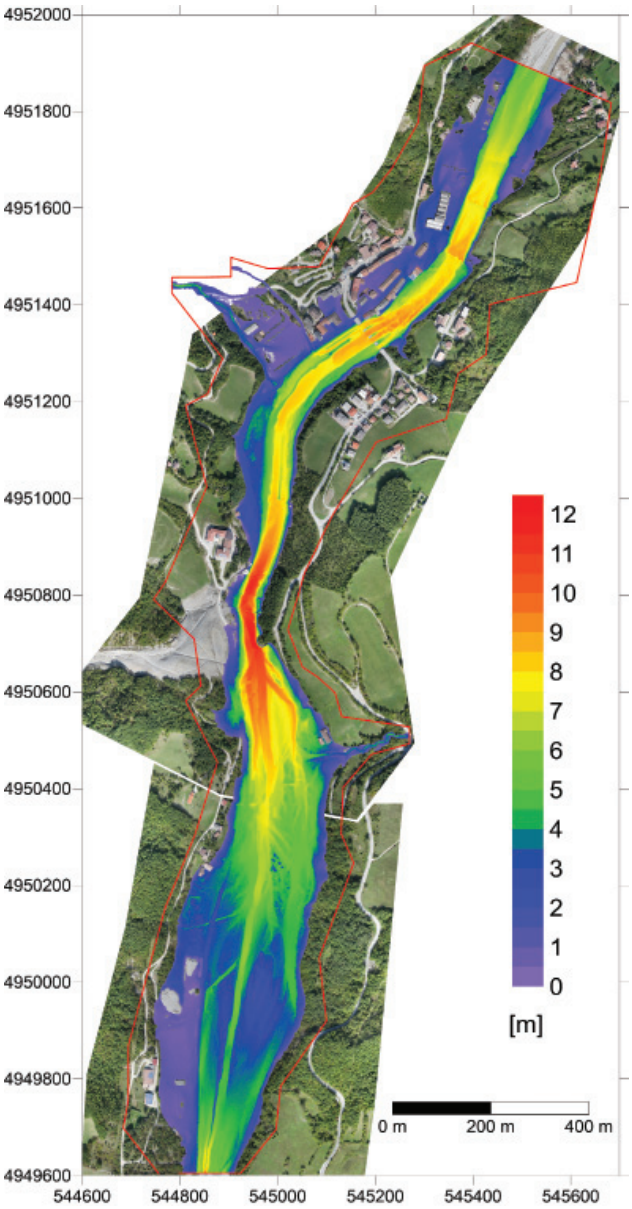

Fig. 19 - Maximum water depths obtained through the numerical simulation

three main tributaries. Downstream, a far-field (zero gradient) boundary condition was imposed. The event was simulated from 11:00 p.m. of September 13th to 4:00 p.m. of the next day, for a total duration of 5 hours. Thanks to the GPU implementation, the simulation runtime was about 1.54 hours adopting a NVIDIA Tesla® K40 device.

Figure 19 shows the contour map of the maximum computed water depths (non-simultaneous). These results can be profitably compared with the data achieved through the post-event surveys. Just upstream the narrowing of the river valley,

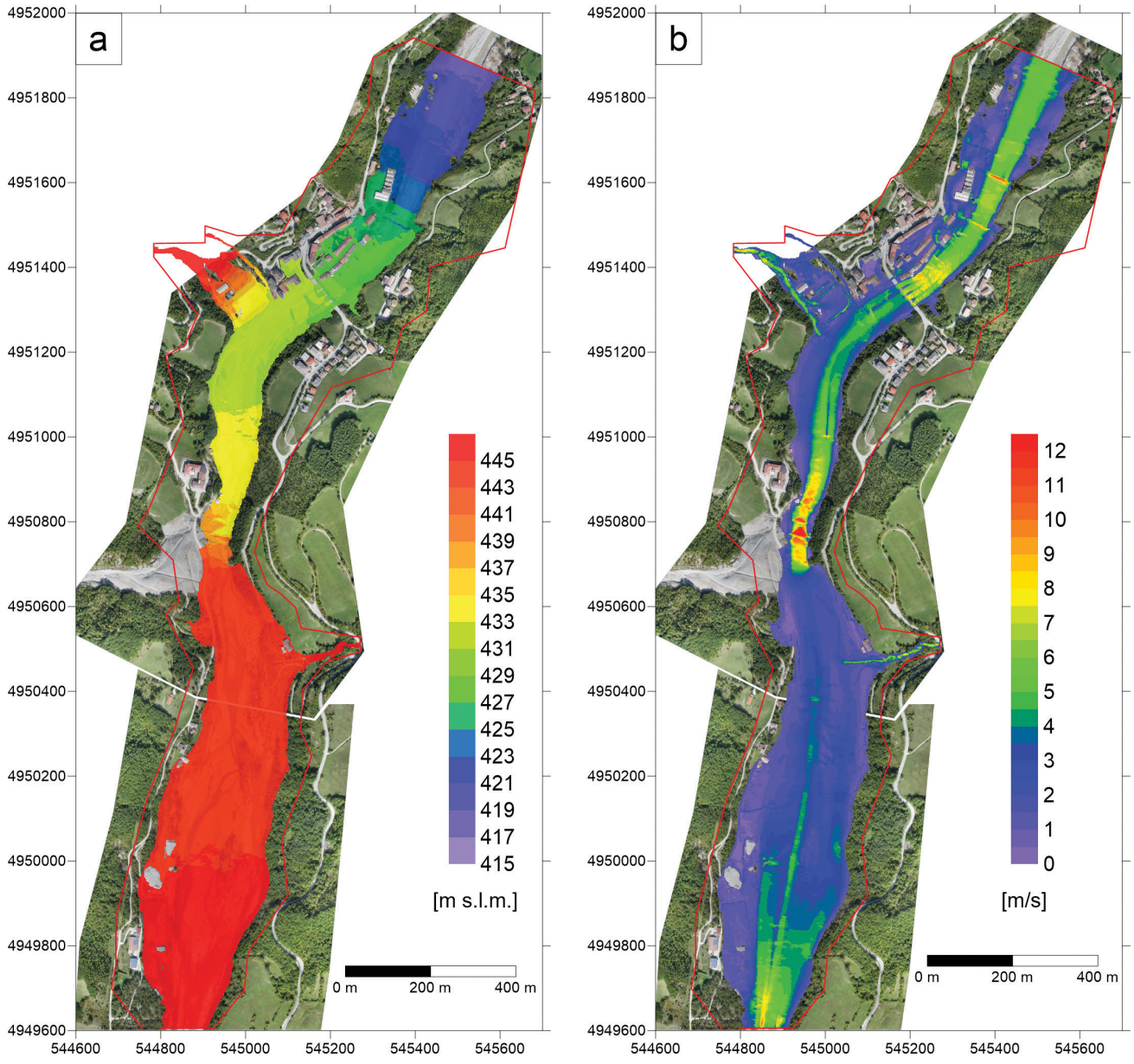

Fig. 20 - Computed water levels (a) and modulus of water velocity (b) at the peak of the flood wave

where the Sassi Neri check dams is located, the computed maximum water depths (up to 11 m) are in good agreement with the observations. Upstream, during the peak of the flood event, the calculated water surface elevation (Fig. 20a) is almost horizontal and the velocity (Fig. 20b) very low, showing clearly that an ephemeral lake formed here, storing an estimated water volume of about $0.9 \cdot 10^6$ m^3.

The numerical results confirm that the two Sassi Neri check dams were completely submerged and circumvented to the left, as confirmed by the side erosion, and by the damages to the structure and to the cradles observed immediately after the event (Fig. 16). Downstream of the valley bottleneck, originated by the presence of the landslide, the flow accelerated and became supercritical with maximum velocities of more than 10-11 ms^{-1}. The velocity then reduces to 5-7 ms^{-1} down to the bridge in Farini (Fig. 20b).

Figure 21 shows a detail of the maximum computed water depths in the center of Farini. The computed values are in very good agreement with the marks left by the waters on the buildings and with the observations acquired during the post-event survey.

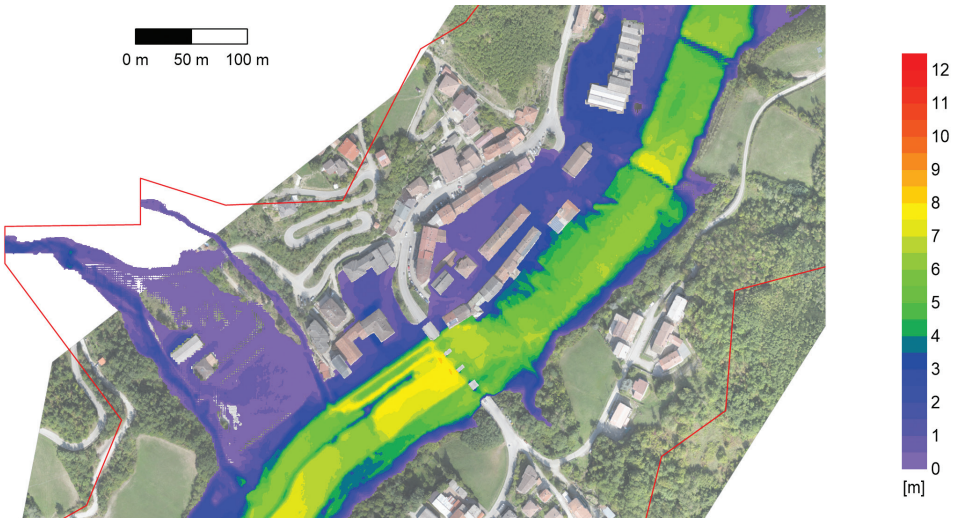

Fig. 21- Detail of the computed maximum water depths at Farini

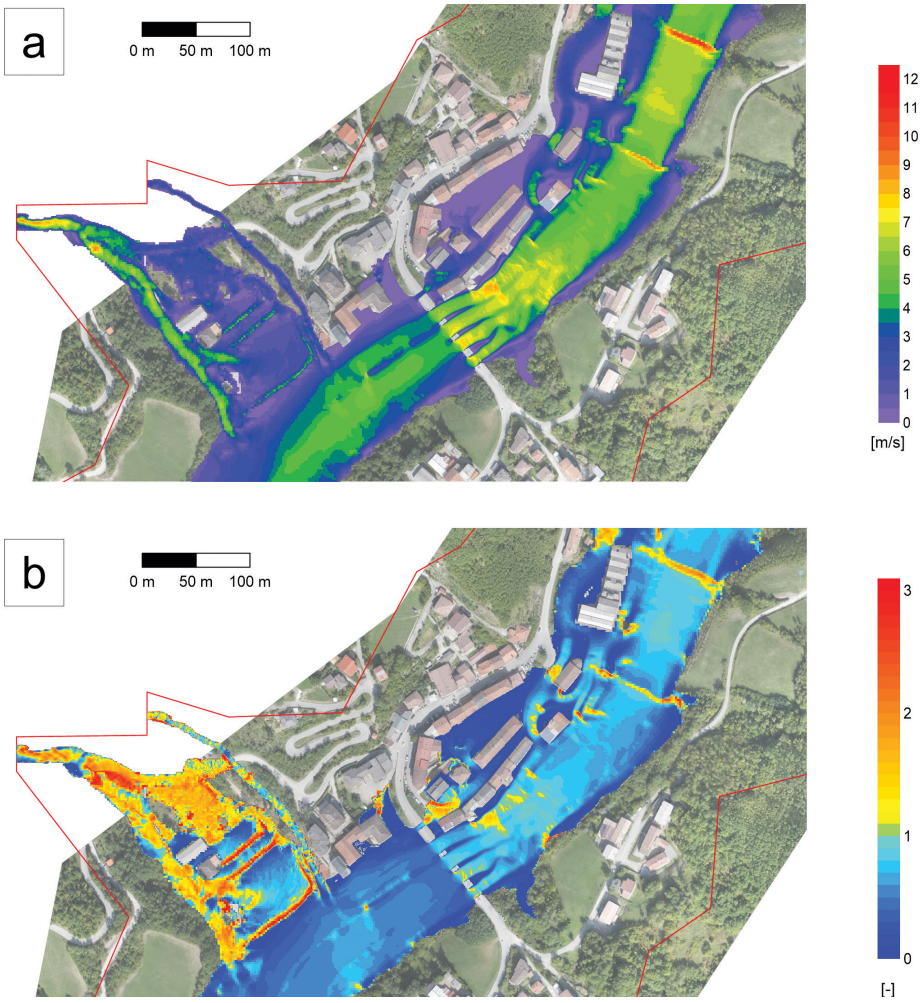

Fig. 22 - Details of computed water velocity magnitude (a) and Froude numbers (b) at the peak of the flood wave in Farini

Figure 22a shows the velocity magnitude computed at the peak of the flood event. In the main channel, values up to 8 ms^{-1}, capable of causing the demolition of the more exposed buildings and of the boulder revetment (Fig. 15), are computed. In the urban area, velocities up to 5 ms^{-1} are obtained. Thanks to the adopted computational multiresolution grid, the effect of the bridge piers is also very well accounted for. As can be recognized by the contour map of the Froude numbers at the peak flow (Fig. 22b), many transitions from subcritical to supercritical flow and vice versa occur.

Figure 23 shows the City Hall and the church after the event, and a detail of the map of the computed velocities and water levels in this area is reported in Fig. 24. The complex flow dynamics can be appreciated, as well as the effect produced by the buildings, clearly recognizable by the marks left by the flood on the edge of the City Hall (Fig. 23). Only a high spatial resolution modelling

Fig. 23 - Marks of the waters on the City Hall of Farini. The building, protruding beyond the row of houses in front of the river Nure, was the first to be hit by the flood flow

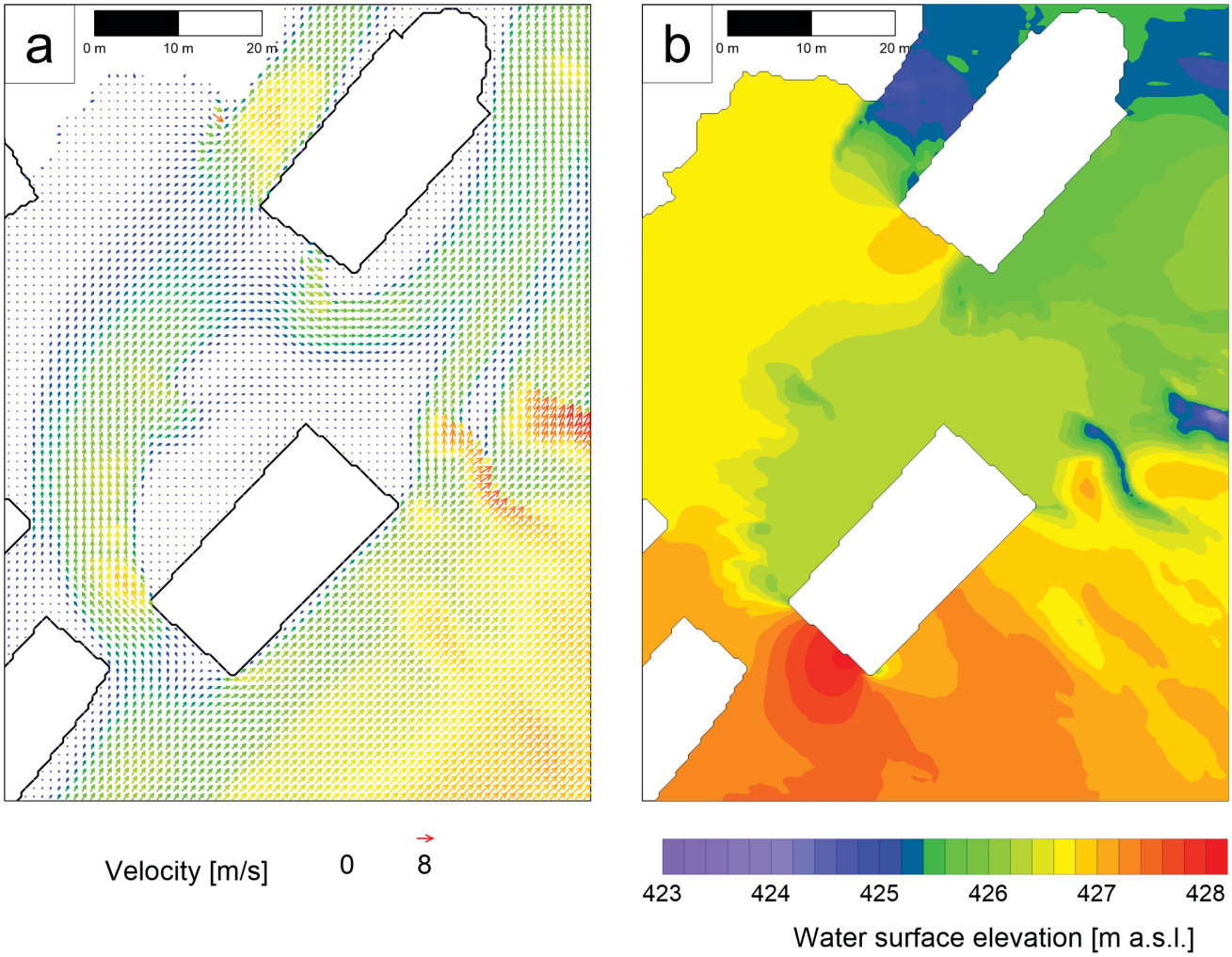

Fig. 24 - Map of the computed velocities (a) and water levels (b) near the City Hall and the church of Fig. 23 (only one velocity vector of two is showed for the sake of visualization)

is capable to account for this kind of features. To evaluate the amount of the inertia terms, that is supposed to be significant due to the abrupt changes in the direction of the flow caused by the buildings (Fig. 23), the corresponding terms in the Saint Venant Equations written in 2D non conservative form were computed:

$$\begin{cases} \dfrac{\partial h}{\partial t} + u\dfrac{\partial h}{\partial x} + h\dfrac{\partial u}{\partial t}x + v\dfrac{\partial h}{\partial t}y + h\dfrac{\partial v}{\partial y} = 0 \\ \dfrac{1}{g}\dfrac{\partial u}{\partial t} + \left[\dfrac{u}{g}\dfrac{\partial u}{\partial x} + \dfrac{v}{g}\dfrac{\partial u}{\partial y} + \dfrac{u}{g}\dfrac{\partial v}{\partial y}\right] + \left[\dfrac{\partial \eta}{\partial x}\right] + S_{fx} = 0 \\ \dfrac{1}{g}\dfrac{\partial v}{\partial t} + \dfrac{v}{g}\dfrac{\partial u}{\partial x} + \dfrac{u}{g}\dfrac{\partial v}{\partial x} + \dfrac{v}{g}\dfrac{\partial v}{\partial y} + \dfrac{\partial \eta}{\partial y} + S_{fy} = 0 \end{cases} \quad (6)$$

Figure 25 shows the contour maps of the inertia terms (first square bracket of eq. 6b) together with the slope of the water surface (second square bracket of eq. 6b). Values of the same order of magnitude, higher than 0.1, are present in both maps. This confirms that neglecting the inertia terms would in this case introduce unacceptable approximations in the numerical solution.

CONCLUSIONS

The simulation of rapidly varying real flooding scenarios can nowadays be satisfactorily performed through high spatial resolution 2D models, thanks to the increasingly widespread and affordable LiDAR DTMs. For this kind of simulations, the computational time has always represented a constraint. The new multiresolution models, such as the one here presented, implemented in a CUDA/C++ code that exploits parallel computation offered by GPU video cards, allow to simulate flooding on wide regions maintaining at the same time a high spatial resolution in the most interesting areas, with very satisfactory ratios of simulation to physical times.

The two test cases considered allowed to assess the good

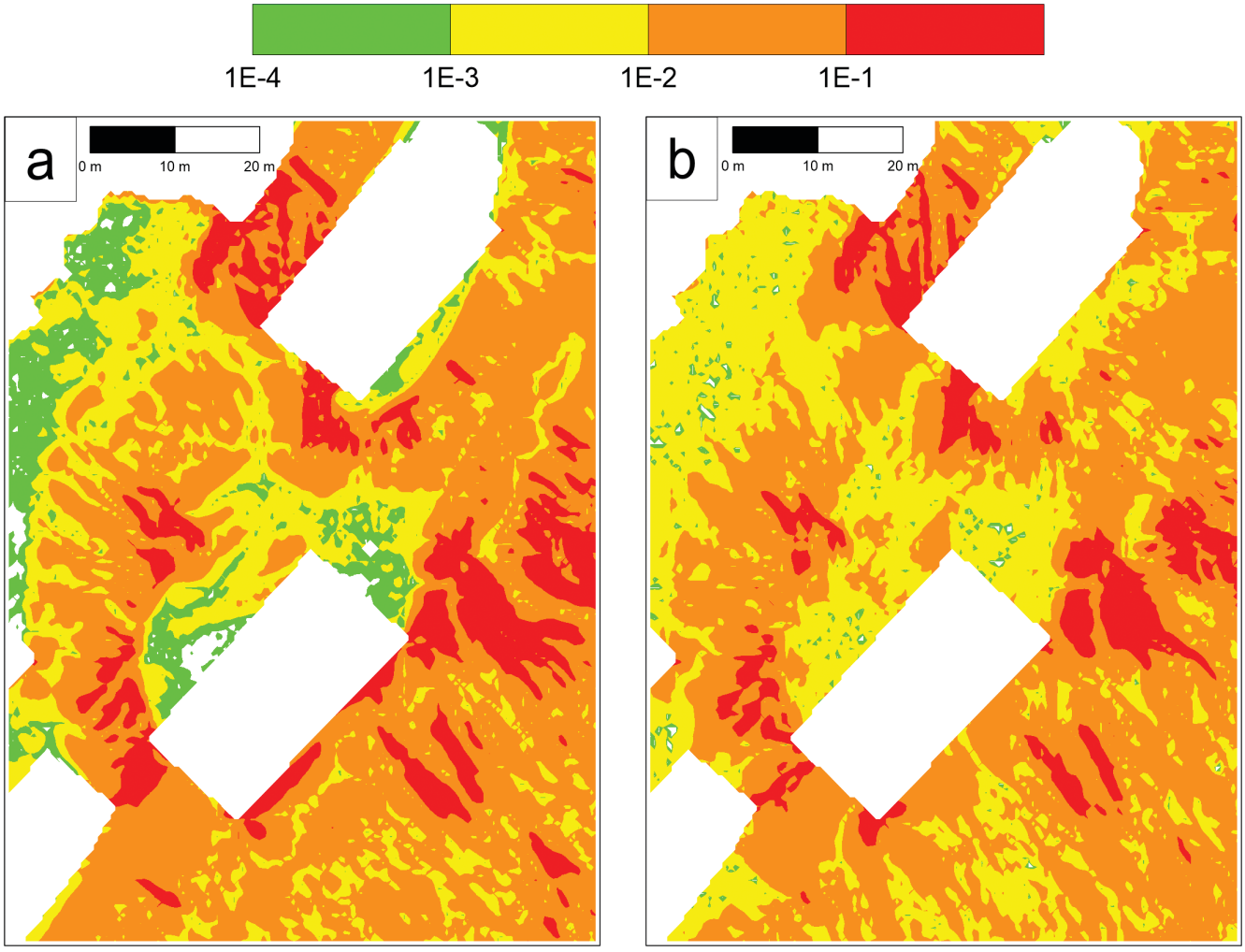

Fig. 25 - Map of the inertia terms (first square bracket in eq. 6b) and of the slope of the water surface (second square bracket in eq.6b) near the City Hall and the church of Fig. 23

predictive skills of the adopted model with regard to the inundations caused by two right tributaries of the Po river in Emilia-Romagna (northern Italy). Both the flood events occurred in densely populated areas and caused huge damages to the urban settlement and infrastructures. The results of the simulations were validated against several field data and observations, with satisfactory results especially in the description of those phenomena that can be correctly modelled only through the adoption of a complete 2D model. Flood inundations in areas characterized by the presence of roads, railways or channel embankments, or in urban environments, where the flooding dynamics can be strongly influenced by streets and buildings, can in fact be correctly simulated only preserving all the terms of the momentum equations. Care has obviously to be taken to achieve an accurate description of these terrain features.

As a matter of fact, flood management in populated territories crossed by rivers is a crucial issue for multiple reasons. On one side, the trend in flood frequency appears to be increasing with a continued worsening of the hydrological inputs; moreover, it has to be considered that, in all likelihood, highly urbanized domains in Europe are usually rich in history and highly productive. For these reasons fast and accurate numerical models, like the one here presented, can be adopted to perform simulations of hypothetical flooding scenarios for flood protection purposes, to evaluate the performances of realized flood detention structures or to investigate the behavior of new flood protection hydraulic structures. The performances of this model can be further improved thanks to the implementation of a Local Time Stepping strategy (Dazzi *et alii*, 2018), or the extension of the code to multi-GPUs.

ACKNOWLEDGMENTS

This work was partially supported by Ministry of Education, Universities and Research under the Scientific Independence of young Researchers project, grant number RBSI14R1GP, CUP code D92I15000190001m. The authors gratefully acknowledge the support of NVIDIA for providing support under the CUDA Research Center Program and the support of INdAM - GNCS Project 2016. Interregional Agency for the Po River (AIPo) is also gratefully acknowledged for providing a copious amount of field data, as well as the Technical Basin Service (STB) of Emilia-Romagna and Dr. Pier Paolo Alberoni of ARPAE (ER).

REFERENCES

Altinakar M.S., McGrath M.Z., Ozeren Y. & Miglio E. (2009) - *Two-sided cut-cell boundary method for simulating linear terrain features and 1D stream flows on a 2D rectangular mesh*. Proc. 33rd Int. IAHR Congress.

Aureli F. & Mignosa P. (2004) - *Flooding scenarios due to levee breaking in the Po river.* Water Management, **157**: 3-12.

ARPAE Servizio Idro Meteo Clima, Servizio Sismico, Geologico e dei Suoli (2016) - *Rapporto sull'evento alluvionale del 14 settembre 2015 (in italian).* www.arpae.it/cms3/documenti/simc/relazioni_idrologiche/ report_evento_14_settembre_2015.pdf

Caleffi V., Valiani A. & Zanni A. (2003) - *Finite volume method for simulating extreme flood events in natural channels.* Journal of Hydraulic Research, **41**: 167-177, London, United Kingdom.

Chanson H. (2012, Ed.) - *Tidal bores, aegir, eagre, mascaret, pororoca*. World Scientific Publishing Co., Singapore, ISBN-13 978-981-4335-41-6

Costabile P. & Macchione F. (2015) - *Enhancing river model set-up for 2-D dynamic flood modelling*. Environmental Modelling & Software, **67**: 89-107, Amsterdam, Netherlands.

Cunge J.A., Holly F.M. & Vervey A. (1980) - *Practical aspects of computational river hydraulics.* Pitman Publishing Limited, London (reprinted by and available from Institute of Hydraulic Research, College of Engineering, The University of Iowa, USA).

Dazzi S., Vacondio R., Dal Palù A. & Mignosa P. (2018) - *A local time stepping algorithm for GPU-accelerated 2D shallow water models*. Advances in Water Resources, **111**: 274-288, Amsterdam, Netherlands.

DICATEA Università degli Studi di Parma (2008) - *Prove su modello fisico del manufatto regolatore della cassa di espansione sul torrente Parma.* In italian, contact the corrisponding author.

D'Oria M., Mignosa P. & Tanda M.G. (2012) - *Reverse level pool routing: comparison between a deterministic and a stochastic approach*. Journal of Hydrology, 470, 28 38, ISSN: 0022-1694, Doi: 10.1016/j.jhydrol.2012.07.045.

Fornasiero A., Amorati R. & Alberoni P.P. (2008) - *Radar quantitative precipitation estimation at Arpa-Sim: a critical approach to retrieve the rainfall rate at the ground level.* Proc. 5th European Radar Conference, 30, Helsinki.

Hylab-DICATeA (2014) - *Videos showing the evolution of the 2D and 3D flooding of Parma* at: www.youtube.com/watch?v=fOZZ8wQHx1E and www.youtube.com/watch?v=0CfERHApvQA

Lacasta A., Morales-Hernandez M., Murillo J. & García- Navarro P. (2014) - A*n optimized GPU implementation of a 2D free surface simulation model on unstructured meshes*. Advances in Engineering Software, **78**: 1-15. http://dx.doi.org/10.1016/ j.advengsoft.2014.08.007

Lacasta A., Juez C., Murillo J. & García- Navarro P. (2015a) - *An efficient solution for hazardous geophysical flows simulation using GPUs*. Computers and Geosciences, **78**: 63 72. Amsterdam, Netherlands. Doi: 10.1016/j.cageo.2015.02.010

Lacasta A., Morales-Hernandez M., Murillo J. & García- Navarro P. (2015b) - *GPU implementation of the 2D shallow water equations for the simulation*

of rainfall/ runoff events. Environmental Earth Sciences, **74** (11): 7295-7305, Springer Berlin Heidelberg. Doi: 10.1007/ s12665-015-4215-z

Liang Q. & Borthwick A.G.L. (2009) - *Adaptive quadtree simulation of shallow flows with wet-dry fronts over complex topography.* Computer & Fluids, **38**: 221-234, Amsterdam, Netherlands.

Liang Q. & Marche F. (2009) - *Numerical resolution of well-balanced shallow water equations with complex source terms.* Advances in Water Resources, **32** (6): 873-884, Amsterdam, Netherlands.

Juez C., Lacasta A., Murillo J. & García- Navarro P. (2016) - *An efficient GPU implementation for a faster simulation of unsteady bed-load transport.* Journal of Hydraulic Research, **54** (3): 275-288, London, United Kingdom. Doi: 10.1080/00221686.2016.1143042.

Miglio E., Altinakar M.S. & Fijolek E.K. (2008) - *Representation of linear terrain features in 2D free surface models using ghost-fluid method.* Proceedings of 8th World Congress on Comp. Mech.(WCCM8) and 5th European Congress on Comp. Meth. in Appl. Sciences and Engrg (ECCOMAS 2008), Venice, Italy.

Mignosa P., Aureli F., Ferrari A., Prost F. & Vacondio R. (2015) - *Approfondimenti idrologici - idraulici a seguito dell'evento alluvionale del 13-14 settembre 2015 nel territorio del comune di Farini, a supporto delle modifiche all'attuale assetto difensivo.* DICATeA, Università degli Studi di Parma (in italian, contact the corresponding author).

NVIDIA CUDA (2007) - *Compute unified device architecture programming guide*.

Raber G.T., Jensen J.R., Schill S.R. & Schuckman K. (2002) - *Creation of digital terrain models using an adaptive Lidar vegetation point removal process.* Advances in Water Resources, **41**: 1-17, Amsterdam, Netherlands.

Ritter A. (1892) - *Die fortplanzung der wasserwellen.* Vereine Deutcher Ingenieure Zeitswchrift, 36, 947 954.

Sampson C.C., Fewtrell T.J., Duncan A., Shaad K., Horritt M.S. & Bates P.D. (2012) - *Use of terrestrial laser scanning data to drive decimetric resolution urban inundation models.* Photogrammetric Engineering & Remote Sensing, **68** (12): 1307-1315, Elsevier, Netherlands.

Schubert J.E. & Sanders B.F. (2012) - *Building treatments for urban flood inundation models and implications for predictive skill and modeling efficiency.* Advances in Water Resources, **41**: 49-64, Amsterdam, Netherlands.

Toro E. (1999a) - *Shock capturing methods for free surface shallow water flows.* Wiley, New York

Toro E. (1999b) - *Riemann solvers and numerical methods for fluid dynamics.* Springer Berlin Heidelberg.

Vacondio R., Dal Palù A. & Mignosa P. (2014) - *GPU-enhanced finite volume shallow water solver for fast flood simulations.* Environmental Modelling & Software, **57**: 60-75, Amsterdam, Netherlands. Doi: /10.1016/j.envsoft.2014.02.003

Vacondio R., Aureli F., Ferrari A., Mignosa P. & Dal Palù A. (2016) - *Simulation of the January 2014 flood on the Secchia River using a fast and high-resolution 2D parallel shallow-water numerical scheme.* Natural Hazards, **80** (1): 103-125, Springer Berlin Heidelberg.

Vacondio R., Dal Palù A., Ferrari A., Mignosa P., Aureli F. & Dazzi S. (2017) - *A non-uniform efficient grid type for GPU-parallel shallow water equations models*. Environmental Modelling & Software, **88**: 119 137, Amsterdam, Netherlands. Doi: /10.1016/j.envsoft.2016.11.012

Valiani A., Caleffi V. & Zanni A. (2002) - *Case study: Malpasset dam-break simulation using a 2D finite volume method.* Journal of Hydraulic Engineering, **128** (5): 460 472.

Vázquez-Cendón M.E. (1999) - *Improved treatment of source terms in upwind schemes for the shallow water equations in channels with irregular geometry.* Journal of Computational Physics, **148** (2): 497 526, Amsterdam, Netherlands.

Received April 2017 - Accepted November 2017